# Prediction of Service Life Decline of Double Welded Wide Flanges due to Fatigue in Steel Arch Bridge under Excessive Loads

**Rusandi Noor[1,*] & Muhammad Noor Asnan[2]**

[1]Structural Engineering Research Group, Departement of Civil Engineering, Universitas Muhammadiyah Kalimantan Timur, Jalan Ir. H. Juanda No. 15, Samarinda 75124, Indonesia
[2] Material Engineering Research Group, Departement of Civil Engineering, Universitas Muhammadiyah Kalimantan Timur, Jalan Ir. H. Juanda No. 15, Samarinda 75124, Indonesia
*E-mail: rn903@umkt.ac.id

**Abstract.** The purpose of this study was to investigate the characteristics of the rate of fatigue fracture propagation in members under maximum force on a steel arch bridge and to identify the fatigue life of those members under excessive loads. The method for bridge fatigue prediction used was numerical S-N curve controlled by cumulative damage rule, fracture critical member, and fatigue fracture determination based on SNI 1729-2015, S-N category. The distribution of stress, strain and life cycle was obtained. The result revealed 1 critical built-up weld beam on the steel arch bridge, specifically double welded wide flange beam TB7. Excessive loads from heavy vehicles, namely trailer types 7C1, 7C2 and 7C3, were simulated. Initial fracturing would occur after 53 years and 5 months of service with an initial crack size of 1.717 mm, leading to a propagation cycle of 45 years, which would cause critical fractures of 10.55 mm after 99 years. Thus, the maximum number of vehicles permitted to enter the bridge, assuming a 5% increase per year, was 13,450 per year for trailer type 7C3 at a planned capacity of 6,984,000 vehicles. This paper illustrates how fatigue life prediction can be a useful guide for the sustainability of bridges and provide a theoretical basis for developing optimized fatigue life of steel arch bridges.

**Keywords:** *bridge fatigue; excessive loads; fracture scheme; life decline; steel arch bridge.*

## 1    Introduction

Bridges as transport infrastructure have a large number of manned vehicles passing over them. Thus, bridge safety directly affects many people's lives. Moreover, in Indonesia, there are many vehicles with excessive loads passing over bridges, which could accelerate damage to bridges as well. Excessive loads on a bridge occur when the number of vehicles that carry loads exceeds the tolerance limit stated in the *Circular Letter on Maximum Limit Guidelines of JBI and JBKI*, Department of Transportation 2008. Damage caused by

overloading can lead to breakdown of a bridge before its technical lifetime is reached, which causes additional costs for bridge maintenance [1]. Fatigue is a condition that makes metals or ductile materials collapse, governed by repeated transient loads over a relatively long time [1]. As a consequence, there will be fractures in the metal, starting with small cracks that become bigger and eventually cause collapse. Fatigue can occur in low force conditions; even 30% of melting stress can cause fatigue [2].

In this study, we analyzed an entire main arch bridge beam using the influence line method with constant amplitude load fluctuation (CALF) limits [2]. As constraint, CALF was used with more dominant load characteristics to tensile load R (stress ratio) R = -1/3 [2]. A fatigue analysis was conducted to determine the damage factor index (D) of a bridge structure designed for excessive and normal loads, with a length of 400 m, from direct measurements on the bridge. The maximum axial load of the girders as the output of the structural analysis due to load was collected and then analyzed numerically to determine the most influenced beam using the S-N curve before it was used in linear elastic fracture mechanics (LEFM). Because the stresses at the crack tip are so small in the fatigue problem, the plastic zone is limited and the stress field behavior can be modeled as linear-elastic. Hence, we determined initial fracturing and crack propagation in the bridge structure, which can grow under repeated applications of stress that are large enough in range. Then we used the Palmgren-Miner model of linear elastic fracture mechanics for the prediction of crack growth. From the estimated cracking, we could determine material toughness with coefficient (0.75), which will occur in accordance with the growth of the number of vehicles. Based on crack propagation we could predict the length of the bridge's service life to set the target service life within the scope of this work [2].

## 2    Methodology

Fatigue life can be modeled as a directed and idealized curve (S-N), where S is the effective stress range, which can be developed using Miner's linear fatigue damage relationship [2]. *N* is related to the applied stress range, so it consists of the gross vehicle weight, a function of the fatigue behavior, and cycle loading. Each curve is governed by the influence line method and by the force cycle equation. The constraints used in service life prediction are fracture equations based on the Paris law [3]. Assessment of fatigue effects on an arch bridge is a difficult task because several mechanisms interact in the process. In this research, the strength assessment derived from stresses or strains in the vicinity of the initial fracture location was a local approach [3]. The local stresses or strains can be obtained from numerical modeling. In a local approach, local fatigue damages such as fracture initiation, crack propagation and final fracture

can be considered [4]. The initial stage of fracturing and crack propagation in the metal fatigue mechanism requires a specified time related to the fatigue life of the component or metal, determined through three stages, as shown in Figure 1.
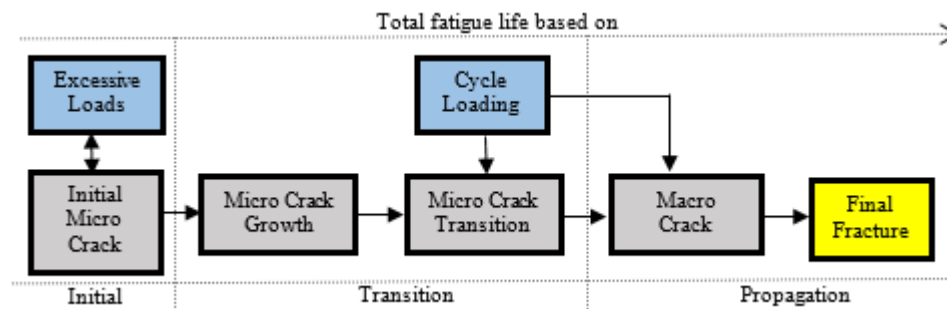


**Figure 1** Description of the fatigue deterioration process in bridges.

In ductile metals the cracking process occurs easily in the initial stage but becomes more difficult in the crack propagation stage [5]. On the other hand, brittle metals are more resistant to initial crack formation but less resistant to crack propagation [5]. The first sub-stage encompasses the time from the end of construction until micro cracks start to appear. For the assessment in this stage, a formulation for vehicle modeling is presented that considers the interaction between three physical problems: load type, vehicle speed, and number of vehicles. The transition time following micro cracks is defined as the time at which maximum micro cracks reach a critical value, leading to crack formation [6].

The local approach methodology is represented in Figure 2. The structural model investigated in the present study corresponds to a steel arch highway bridge spanning 400 m, with simple straight-axis support. The procedure used was modeling overloaded heavy vehicle data in real time in a cycle. The initial stage consisted of conducting an analysis to find out the influence line for which beam is most conducive to fatigue. The selected beam was then used as the major input in the analysis of the 3-dimensional finite element model for finding initial micro crack formation and crack propagation in a welded beam. This was the basis for the subsequent analysis based on the concept of accumulation to obtain the value of the damage factor. The primary data used in this research were statistical load data on actual axle loads from several heavy vehicle types from a research conducted by National Road Implementation Region V and structural data from the Bina Marga Service of East Kalimantan province for an steel arch bridge with a total span of 400 m. Structure analysis

was carried out for each combination from any direction of the trailers. This analysis produced a stress value as the output, which was subsequently used to form a stress transfer function to obtain the fracture critical member. The damage factor together with the fracture critical member were used as input for the determination of fatigue cracking. The proposed analysis methodology and procedures, presented in design code, were used to evaluate the bridge fatigue response in terms of its structural service life [7]. The main conclusions of this paper focused on alerting structural engineers to the possible distortions related to a bridge's service life when subjected to vehicle overload [8].
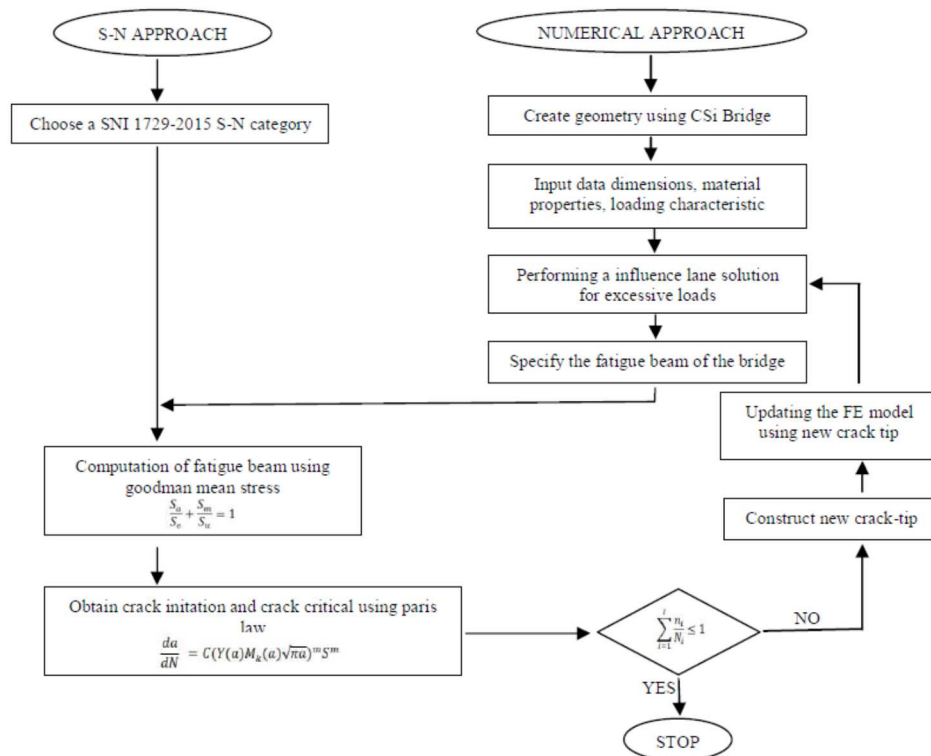


**Figure 2** Local approach of fatigue strength and fatigue life assessment of a steel arch bridge.

## 3    Numerical Model

### 3.1    Arch Bridge Structural Model

The 3D model of the 400-m bridge structure in full scale with CsiBridge included visualization data of the bridge geometry as shown in Figure 3(a)-(c).

The steel sections used were welded wide flanges (WWF) made with 355 MPa yield stress steel grade and 490 MPa ultimate strength. A $2.05 \times 10^5$ MPa Young modulus was adopted for the steel beams. The weld material used was E70XX with 415 MPa yield stress and 495 MPa ultimate strength.
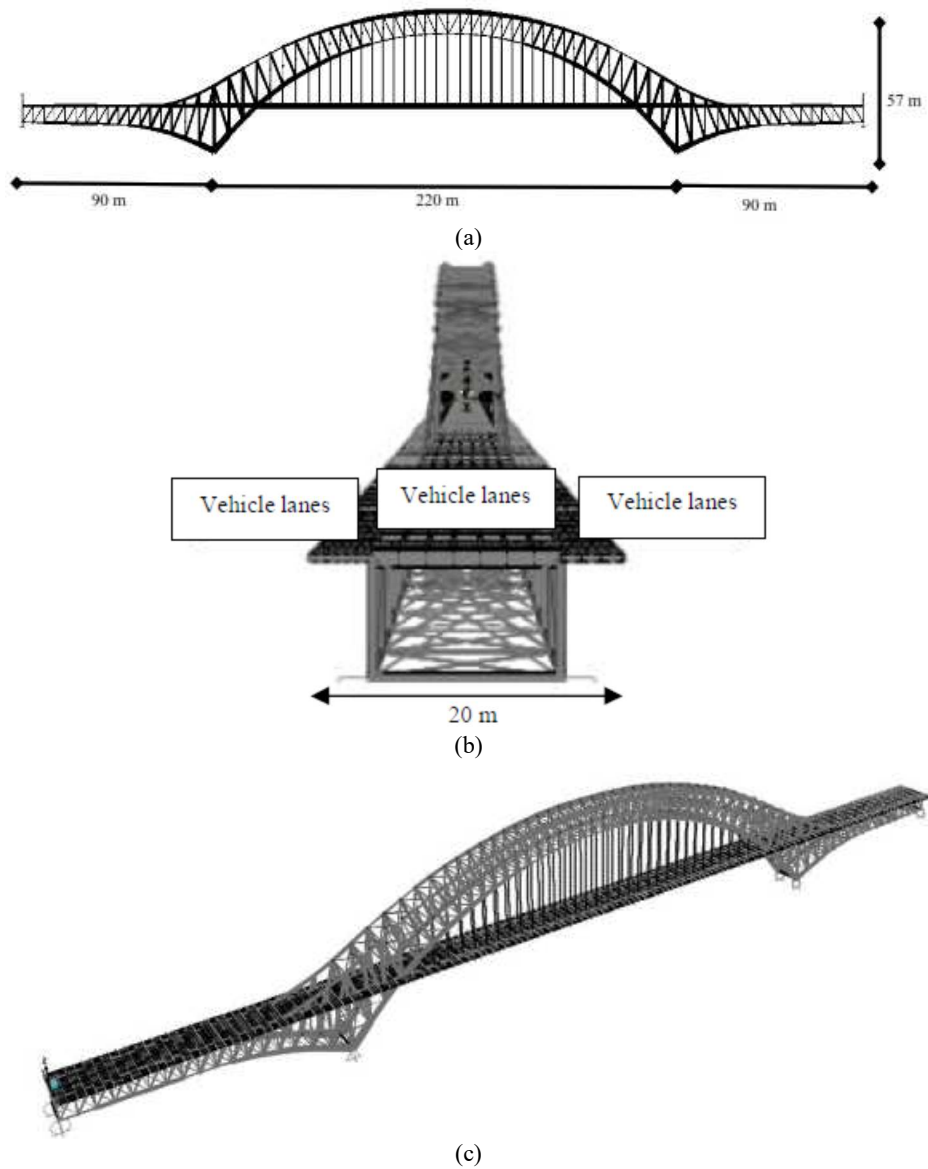


(a)



(b)



(c)

**Figure 3** Bridge model: (a) frontal view, (b) cross section, (c) three-dimensional view.

## 3.2    Stress Variation

The actual load of a vehicle that occurs on the bridge is always different from the standard vehicle load. Any load that passes over the bridge will provide distinctive stress variations on the beam under review [9]. In this study, a normal weight of vehicle load was employed in order to make a comparison of fatigue accumulation on the bridge (see Table 1).

**Table 1**    Heavy vehicle loads.

| Type Axis Configuration | Overload Axis Load (Ton) [10] | | | | Normal Axis Loads (Ton) [11] | | | | Up (%) |
|---|---|---|---|---|---|---|---|---|---|
| | Front | Middle | Back | Total | Front | Middle | Back | Total | |
| Type 7C1 | 7.1 | 15.5 | 34.7 | 57.3 | 6 | 10 | 18 | 34 | 41 |
| Type 7C2 | 6.6 | 13.1 | 45.5 | 65.3 | 6 | 10 | 30 | 46 | 30 |
| Type 7C3 | 7.2 | 21.4 | 44.1 | 72.8 | 6 | 20 | 30 | 56 | 23 |

The source used to determine the actual axle load for each heavy vehicle type was the research by the Office for National Road Implementation Region V conducted in 2007. The results are listed in Table 1. Vehicles that cause variations of stress below 26 MPa do not cause fatigue according to SNI 1729-2015, so they are not included in this calculation. Three actual loads of vehicle axles were simulated on the bridge model. The distance between a pair of axles can be varied within a fixed region. The lanes were only modeled for the movement of the vehicles. The mathematical vehicle model adopted in this work was developed by CsiBridge.
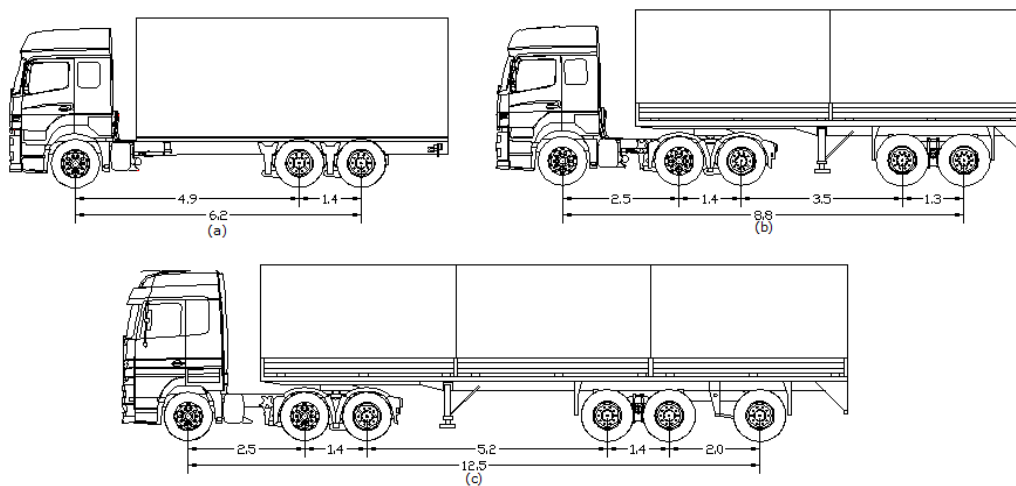


**Figure 4**    Vehicle models (a) trailer type 7C1, (b) type 7C2, (c) type 7C3.

The difference of each type of trailer lies in the length of the cargo carried, with different axis configurations, as presented in Figure 3. In Table 1, it can be seen that the vehicle load exceeds the permitted load limit by 5% per vehicle, so that the behavior allows stress concentration on each member of the bridge. In this study, only certain parts of the elements of the steel arch bridge were analyzed: a certain beam profile that will undergo excessive stress and causes the bridge fatigue service life to decrement [9].

## 3.3    Semi-infinite Train of Vehicles

The moving load was modeled as an infinite series of combination trailers, regularly spaced and running at constant velocity ($u$). If $I$ is the distance between two successive vehicles and as these trailers enter one by one onto the bridge deck, a time-repeated movement variation is created that is governed by frequency $ft = u/I$, associated with the movement of the vehicles over the bridge, which can be called the traversing frequency. After a certain time period ($t_1$), called the crossing period, the first trailer in the train reaches the far end of the bridge and from this instant the total mass of the vehicles on the bridge remains practically constant. Under these conditions the bridge will soon reach a steady-state response situation, which includes repetition of maximum values directly related to the fatigue and service life of the structure, as illustrated in Figures 5(a)-(c).
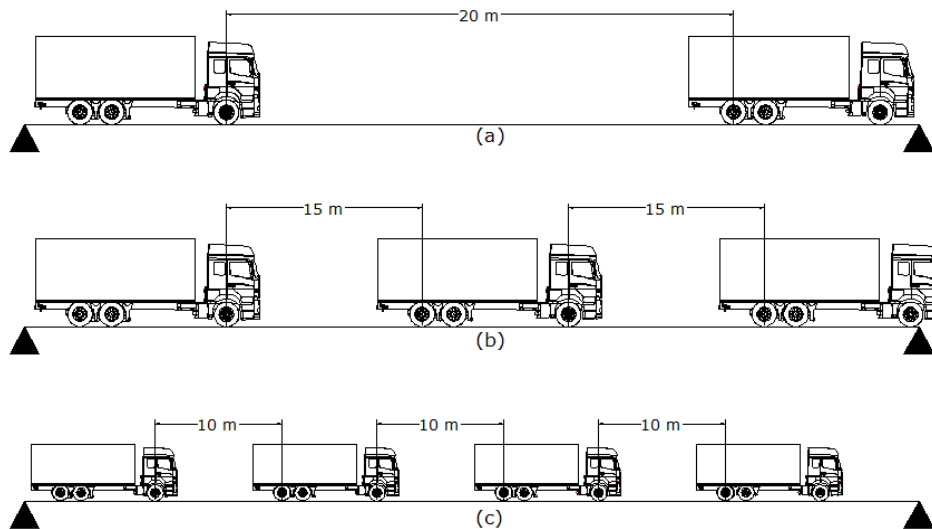


**Figure 5**  (a) Two trailers crossing the bridge: $u = 80$ km/h and $I = 20$ m, (b) three trailers crossing the bridge: $u = 60$ km/h and $I = 15$m, (c) four vehicles crossing the bridge: $u = 40$ km/h and $I = 10$ m.

This applies to all trailer types, so there are 81 combinations of loading on the bridge. Vehicles passing over the bridge during the service period were assumed to have excess load characteristics [9]. The number of passing vehicles was considered proportional to a growth of the number of passing vehicles by 5% per year. The load of the trailers inputted into the modeling shown in Figure 6 was the real load per time according to Table 1.
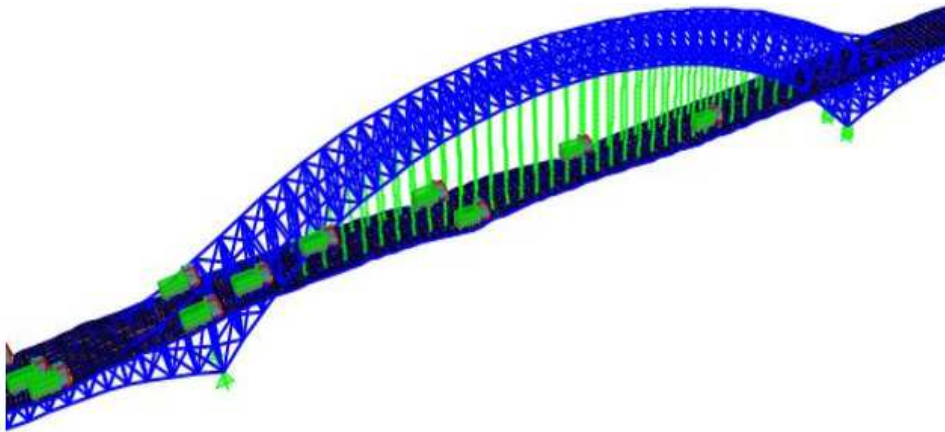


**Figure 6**  Modeling of moving trailers in CsiBridge.

## 4        Fatigue Critical Member

The fatigue critical member (FCM) is a steel bridge component with tensile stress, or with a tensile part, the failure of which will cause partial or complete collapse of the bridge [12]. Determination of the FCM using the method in Section 3.3 makes it possible to see the behavior of the beam trusses in detail one by one. To establish the stress in the bridge section, the influence line was used so that the tensile stress and compress stress on the bridge could be determined [12]. The failure of a beam of a bridge is largely (38.3%) determined by fatigue. The focus of this research was on a welded wide flange beam. In contrast to a profile beam, this type of beam can withstand fatigue [12].

The potential fatigue beam on the bridge was a double welded wide flange TB7 beam, as shown in Figure 7(a), with a tensile stress of 173.55 MPa and 98.9 MPa compressive stress. As shown in Figure 8, it was a double welded wide flange TB7 beam with dimensions of 550 x 450 cm, a 25-mm flange, a 12-mm web, and a length of 500 cm. On the diagonal beam, as shown in Figure 7(b), the stress occurring above the fatigue requirement of stress was 86.25 MPa.
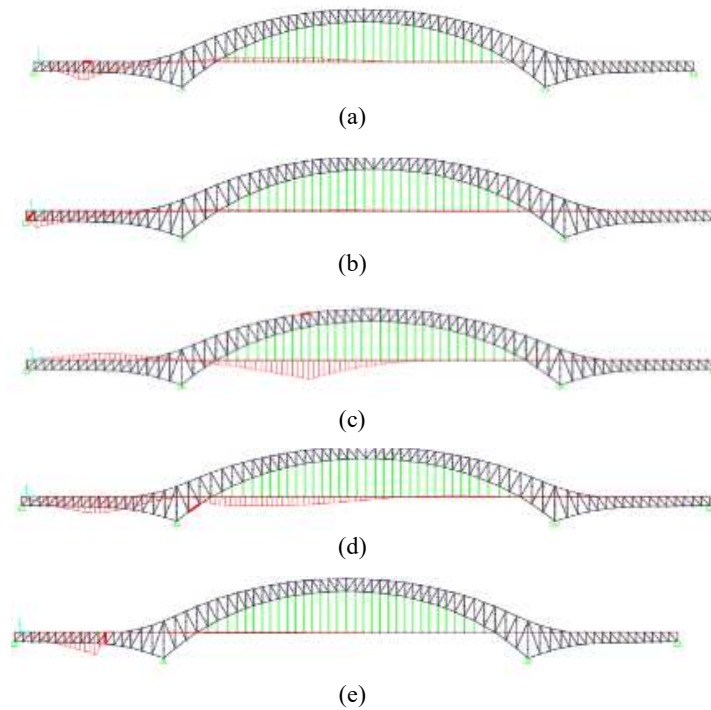
(a)

(b)

(c)

(d)

(e)

**Figure 7** Influence line: (a) TB7 (tie beam), (b) BD1 (diagonal beam), (c) BPA15 (upper curved beam), (d) BPB2 (lower arch beam), (e) BT12 (vertical beam).
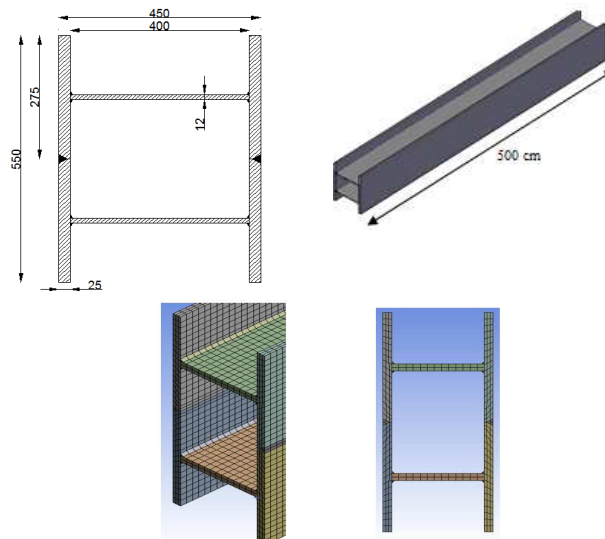


**Figure 8** Double welded wide flange TB7 beam.

## 5      Idealized S-N Curve

The test data for the double welded wide flanges and welded wide flanges are summarized in Figure 9. The stress range is plotted as a function of the life cycle for excessive load levels of minimum stress on a log-log scale [12]. This is readily demonstrated by Figure 9, with the yield stress ranging from 160 MPa to 370 MPa, representing the extremes generally used in bridge construction. The data plotted in Figure 9 clearly show that the stress range is the critical stress variable for all structural steels. The result also confirms the significance of the type of detail. Idealization of the S-N curve made with the help of AnSYS obtained S-N curves that represent excessive trailer load. The result of this modeling was converted to actual force values that occurred on the bridge and changed to the cumulative frequency percentile. After knowing the actual force on the bridge member, the particular part that withholds extreme behavior due to normal load can be seen in Figure 7(a) and due to actual overload in Figure 7(b). The curve is divided into 2 main parts: 1) low-cycle fatigue with 1-1000 or 10000 cycles, 2) high-cycle fatigue with more than 10000 cycles, which can occur on any bridge. At low stress fatigue, the bridge's lifetime is unlimited, which is called the constant amplitude fatigue limit (CALF). For phase 1, when all cycles on the spectrum are above the CALF, the Miner equation was used to determine the stress range equivalent. The second phase, when the stress range is within part of the CALF, is more common in the bridge. In the third phase of stress ranges, occurring under the CALF, there is no fatigue damage [12].
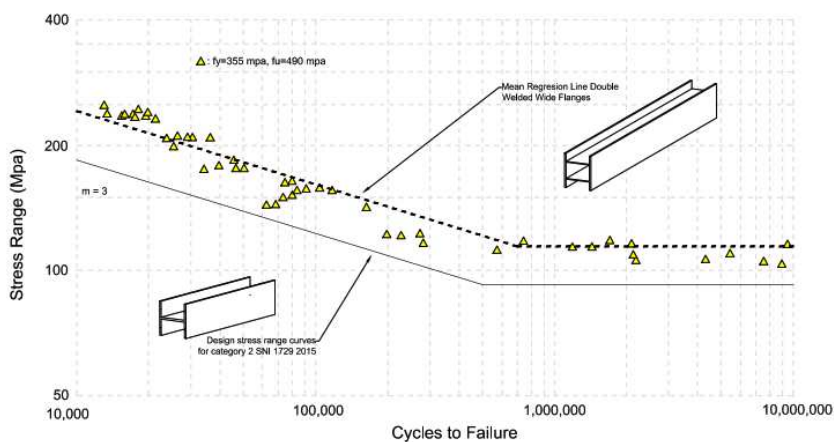


**Figure 9**  Comparison of design stress category 2 SNI 1729 2015 with double welded wide flanges.

Because the fluctuation of the stress-intensity factor is the primary fatigue-crack-propagation force, it can be surmised that the rate of fatigue crack

propagation is governed by the local stress-intensity-factor fluctuation. This means that the fatigue-crack-propagation rate per cycle (*da/dN*) in the shadow of a notch must be governed by Eq. 1 [13].

$$\frac{da}{dN} = A(\Delta K_{eff})^n \tag{1}$$

Eq. (1) can be used to analyze the fatigue-crack growth behavior of cracks emanating from regions of stress concentrations. $\Delta K_{eff}$ is the effective stress intensity factor range, which can be derived from the nominal stress fluctuation ($\Delta \sigma$) and the stress-concentration factor ($k_t(a)$). With the value obtained from the S-N curve of each load on the beam, the damage factor is calculated using the Palmgren-Miner method as expressed in Eq. (2):

$$\sum_{i=1}^{l} \frac{n_i}{N_i} \leq 1 \tag{2}$$

The damage factor influences the vehicle capacity that is allowed onto the bridge every year. Assume that $n_i$ is the cyle load for a particular type of vehicle that enters the bridge. $N_i$ is the cycle obtained from the S-N curve, the damage factor approached with the Palmgren-Miner method assumes that during the lifetime of the bridge trailers will continue to pass over it [14].

## 6      Analysis and Discussion

### 6.1    Damage Factor

In this calculation, the accumulated number of trailers on a typical steel bridge in 2016 was used, which was obtained from data provided by transportation service Samarinda. 7C1 trailers during 2016 accounted for 45,000 vehicles, 7C2 trailers accounted for 21,900 vehicles, and 7C3 trailers accounted for 13,450 vehicles. In the idealization of the S-N curve, the capacity of each vehicle varies. In overload condition, the capacity or cycle of 7C1 trailers was estimated at 17,256,000 vehicles per year, for 7C2 trailers it was 12,421,000 vehicles per year, and for 7C3 trailers it was 6,984,700 vehicles per year. Dividing each cycle of permitted load stress per year by the capacity of the cycle of a specific stress allowed per year, the accumulated damage factor is close to 1, as can be seen in Table 2 [14]. This indicates the bridge safety limit of heavy vehicle loads entering the bridge each year.

After obtaining the number of vehicles allowed per year, the growth of the number of vehicles passing over the bridge per year was set to 5%. This growth is directly related to the crack coefficient that occurs on the bridge, also known

as the critical member fracture [15]. From the accumulated number of vehicles and the permitted stress cycle we got a crack coefficient value of 0.75. In other words, 75% of bridge service life in year 99. For 7C3 trailers, the estimation is about 1,604,256 vehicles per year, for 7C2 trailers it is about 2,612,134 vehicles per year, and for 7C1 trailers it is about 5,367,398 vehicles per year. This value is also a reference to the next calculation, which determines the crack initiation and crack propagation that will occur in the TB7 beam.

**Table 2**    Damage factor.

| 7C1 trailer type | | | 7C2 trailer type | | | 7C3 trailer type | | |
|---|---|---|---|---|---|---|---|---|
| Cap. (Ni) | Stress | DF | Cap. (Ni) | Stress | DF | Cap. (Ni) | Stress | DF |
| 17256000 | 71.74 | 0.0026 | 12421000 | 86.14 | 0.0018 | 6948700 | 115.79 | 0.0019 |
| 9938300 | 75.24 | 0.0045 | 6915400 | 91.08 | 0.0032 | 3799000 | 123.40 | 0.0035 |
| 6063400 | 78.74 | 0.0074 | 4015900 | 96.01 | 0.0055 | 2144000 | 131.01 | 0.0063 |
| 3779600 | 82.23 | 0.0119 | 2393200 | 100.94 | 0.0092 | 1334600 | 138.60 | 0.0101 |
| 2402900 | 85.73 | 0.0187 | 1529000 | 105.88 | 0.0143 | 909410 | 146.21 | 0.0148 |
| 1613900 | 89.22 | 0.0279 | 1021500 | 110.81 | 0.0214 | 700170 | 153.82 | 0.0192 |
| 1129500 | 92.72 | 0.0398 | 797290 | 115.74 | 0.0275 | 545230 | 161.42 | 0.0247 |
| 871450 | 96.21 | 0.0516 | 633400 | 120.68 | 0.0346 | 429020 | 169.03 | 0.0314 |
| 709590 | 99.71 | 0.0634 | 507670 | 125.61 | 0.0431 | 340830 | 176.64 | 0.0395 |
| 581890 | 10321 | 0.0773 | 410240 | 130.54 | 0.0534 | 273170 | 184.24 | 0.0492 |
| 480340 | 106.70 | 0.0937 | 334040 | 135.47 | 0.0656 | 220750 | 191.85 | 0.0609 |
| 398970 | 110.20 | 0.1128 | 273930 | 140.41 | 0.0799 | 186990 | 199.46 | 0.0719 |
| 333310 | 113.69 | 0.1350 | 226120 | 145.34 | 0.0969 | 165010 | 207.07 | 0.0815 |
| 279980 | 117.19 | 0.1607 | 192230 | 150.27 | 0.1139 | 146230 | 214.67 | 0.0920 |
| 236390 | 120.69 | 0.1904 | 171640 | 155.20 | 0.1276 | 130090 | 222.28 | 0.1034 |
| Accumulation = | | 0.9979 | 153780 | 160.14 | 0.1424 | 116160 | 229.89 | 0.1158 |
| | | | 138230 | 165.08 | 0.1584 | 104070 | 237.49 | 0.1292 |
| | | | Accumulation = | | 0.9986 | 93473 | 254.87 | 0.1439 |
| | | | | | | Accumulation = | | 0.9992 |

## 6.2    Determination of Fatigue Crack Value

In this section, the coefficients that affect fatigue cracking are determined, both during initiation and propagation [15]. The stress quantity used was $\Delta\sigma$=173.55 MPa, with a stress intensity factor of $Y(a)$ = 0.99745. The latter value was taken from the assumption that cracks occur in the form of semi-elliptical surface cracks. A validation model was used to determine the intensity stress factor coefficient value of $M(k)$ = 1. The critical crack size was determined with Eq. (3) [13].

$$a_{crit} = \frac{1}{\pi}\left(\frac{K_{IC}}{1.69\sigma_{avr}}\right)^2 \tag{3}$$

From the equation, a critical crack value of 10.06 mm was obtained. Then, the value of crack initiation was determined by performing trials on each specimen in accordance with the cycle that occurs, using Eq. (4) as follow[15]:

$$N_f = \frac{1}{C}\int_{a_{initial}}^{a_{critical}} \frac{da}{(SY(a)M_k(a)\sqrt{\pi a})^m} \tag{4}$$

with $m$ = 3.15 (ranging between 3-5 for steel) and $N_f$ = 1604255 cycles. The crack value obtained was $a_0$ = 1.717 mm. A schematic diagram showing the general relation between fatigue-crack initiation and propagation is shown in Figure 10. The fatigue rate transition scheme shown in Figure 10 is appropriate to represent the mechanical fatigue failure, which starts with micro fractures appearing during the initiation period and ends with macro fractures appearing during the propagation period. In Region 1 it is very difficult to tell if the cracking happened because of micro cracks. In Region 2, cracks can be detected early, but this is still within the estimation phase. For TB7, phase 2 is from cycle 146,891 to 176,762. When converted into years, phase 2 is expected to start in the years 50 to 54 of bridge service. The total service life of the bridge at an estimated 75% of service life in the previous calculation is 99 years for an increase in the number of vehicles by 5%. In the third stage, cracks can be seen clearly and repair can be done to the member. The fatigue rate transition from the behavior in Region 2 to Region 3 can be predicted by using Equation 5 [13]. The stress intensity factor value ($K_T$), which defines this transition region under zero to tension loads can be calculated with an equation taken from [14], in the following form:

$$K_T = 0.04\sqrt{E\sigma_{ys}} \tag{5}$$

Eq. (5) was used to calculate the stress-intensity-factor value corresponding to onset of fatigue-rate transition $K_T$, which also corresponds to the point of transition from Region 2 to Region 3 in materials that have high fracture toughness. Moreover, extrapolation of the behavior in Region 2 to $K_{IC}$ values that are higher than $K_T$ could seriously overestimate the useful fatigue life of structural components. Accurate prediction of finite fatigue lives of structural components is subject to high stress fluctuations, requiring an exact characterization of fatigue-crack-growth behavior above and below the fatigue transition region. Determining the location of crack initiation in the TB7 beam by applying the maximum stress concentration vector principle, it can be estimated that crack initiation will occur where the web and flange meet, as shown in Figure 11. For those cases where fatigue crack growth is a

consideration, for example in bridges, the total useful design life of a structural component can be estimated from the time it takes for cracks to grow from sub-critical dimensions to critical size. In an engineering sense, the initiation stage is the region where fatigue cracks propagate. The sub-critical crack growth stage is the region where a propagating fatigue crack follows one of the existing crack growth laws according to Eq. (1). The unstable crack growth stage is the region where either fatigue crack growth is very rapid, or brittle fractures occur, or ductile tearing.
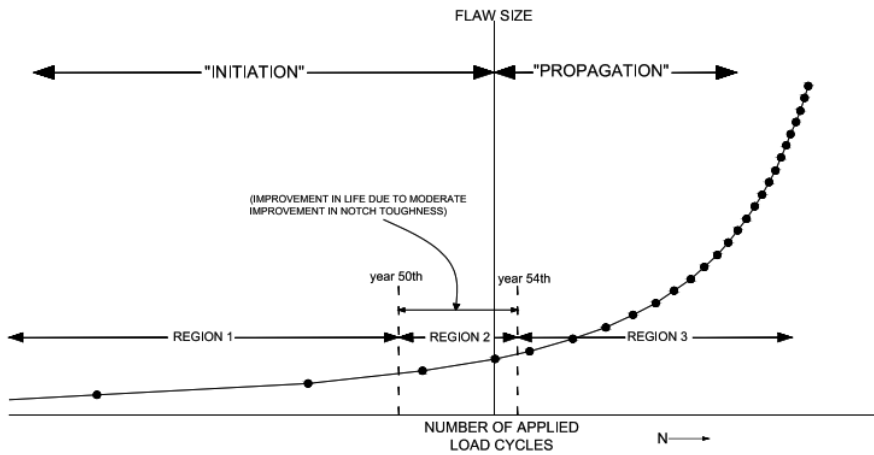


**Figure 10**    Schematic showing the relationship between crack initiation life and crack propagation life of the double welded wide flange beam.
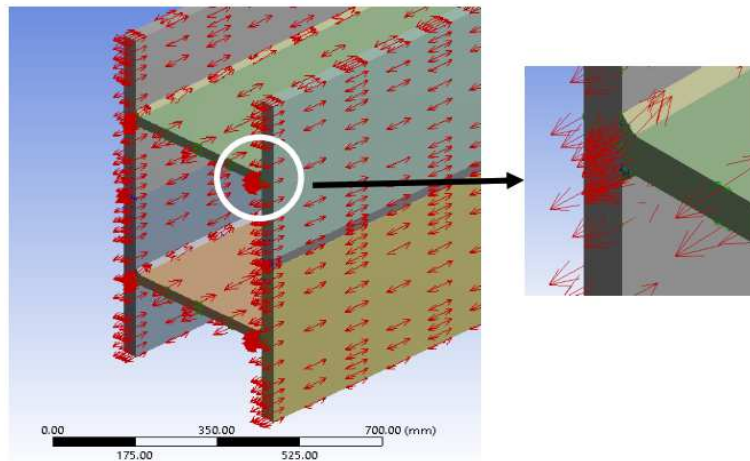


**Figure 11**    Assumption of location of cracks in welded wide flange beam.

Validating the cycle against the initial estimate using the crack growth rate with Eq. (7) [15]:

$$K_I = 2\sigma M_k \left(\frac{a}{Q}\right)^2 \tag{7}$$

and estimating $\frac{a}{2c}$ = 0.3688, $\frac{\sigma}{Sy}$ = 0.5, and Q with graph 1.75, we get = 29.57

MPa. Thus, we know that the crack growth value is 9.3107543568927E-06 mm/cycle. The fracture design criteria are based on the maximum stress obtained from the S-N curve divided by the safety factor in the range of the yielding stress of the material itself. The stress reduction coefficient for steel is determined at 0.717. From the fracture analysis on the S-N curve, a fractional stress of 629 MPa was obtained. When viewed from the limit of the yielding stress of the material ($Fy$ = 355 MPa) and the stress to reach fracture ($Fcr$ = 629 MPa) for the profile thickness in the estimated area a 25-mm crack will appear. In such circumstances it is certain that the failure that occurs will be dominantly yielding. However, this will never happen because before fractures can occur there will have been a material yield failure.
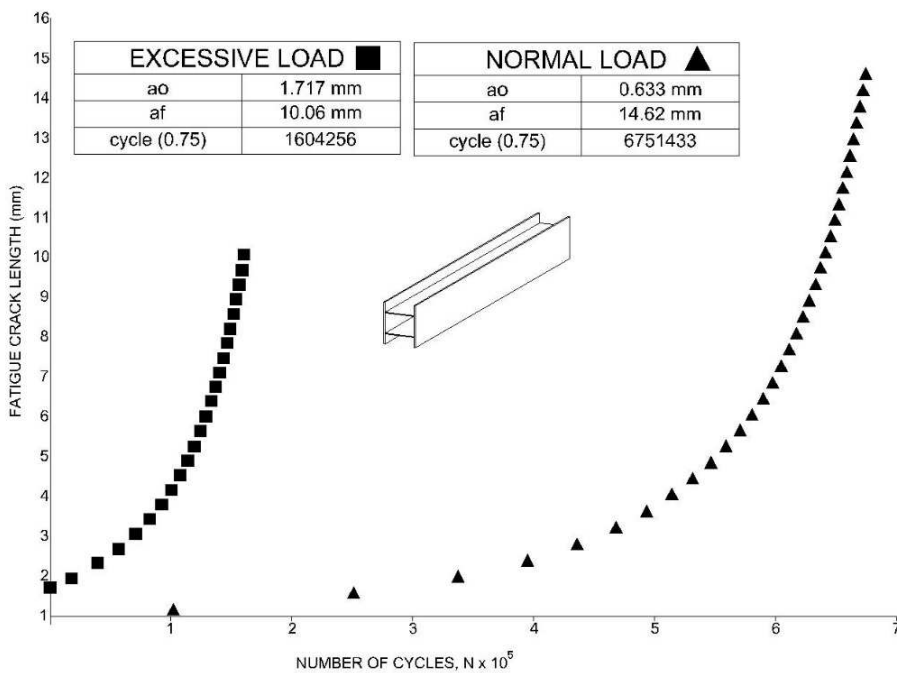


**Figure 12**   Effect of initial crack length on crack growth.

According to the schematic of material toughness of steel is 50 MPa $\sqrt{m}$ when it reaches cycle 1,604,255, or service year 99. With a crack coefficient equal to 0.75, the material toughness value is equal to 40 MPa $\sqrt{m}$, i.e. 81.699% of the total toughness value. Material toughness at cycle 172,848, or at crack $K$, is equal to 29,572 MPa $\sqrt{m}$, or 59.141%. The comparison can be seen in Figure 12.

## 7    Conclusion

Initial fatigue cracks appear in year 54 of service with a size of 1.717 mm and critical cracks appear in year 99 at 10.55 mm. The number of stress cycles allowed to pass the bridge with a growth of 5% for trailer type 7C1 is 45,000 maximum per year with a planned capacity of 17,256,000 vehicles; for trailer type 7C2 it is 21,900 maximum per year with a planned capacity of 12,421,000 vehicles, and for trailer type 7C3 it is 13,450 maximum per year with a planned capacity of 6,984,000 vehicles. This means a service life decline of 24 years compared to normal vehicle loads that pass over the bridge. Initial cracks due to normal vehicle loads will occur in service year 78 of the bridge, with a size of 0.628 mm and critical cracks of 14.629 mm will appear in service year the 117.

## Acknowledgments

## References

[1]    AASHTO, *AASHTO LRFD Bridge Design Specification 6th ed., Section 3, American Association of State Highway and Transportation Official, Washington DC, USA*, pp. 17-36, 2012.

[2]    Mei, J. & Dong, P., *An Equivalent Stress Parameter for Multi-axial Fatigue Evaluation of Welded Component Including Non-proportional Loading Effect,* International Journal of Fatigue, **101**, pp. 297-311, 2017.

[3]    Paris, P.C. & Erdogan, F., *A Critical Analysis of Crack Propagation Laws,* J. Basic Eng. **85**(4), pp. 528-534. 1963.

[4]    Soliman, M., Frangopol, D.M. & Kown, K., *Fatigue Assesment and Service Life Prediction of Exisisting Steel Bridge by Using a Bilinear S-N Approach,* Journal of Bridge Engineering, **17**(1), pp. 58-70, 2012.

[5]     Aygul, M., Al-Emrani, M. & Urushadze, S., *Modelling and Fatigue Life Assessment of Orthotropic Bridge Deck Details Using FEM*, International Journal of Fatigue, **40**, pp 129-142, 2012.

[6]     Sonsino, C.M., *Multiaxial Fatigue Assesment of Welded Joints-Recommendations for Design Codes*, International Journal of Fatigue, **31**(1), pp, 173-187, 2009.

[7]     Zhang, G. & Richter, B., *New Approach to the Numerical Fatigue-Life Prediction of Spot-welded Structure*, Fatigue and Fracture Engineering Materials and Structure, **23**(6), pp. 499-508, 2000.

[8]     Xiao, Z.G. & Yamada, K., *A Method of Determining Geomteric Stress for Fatigue Strength Evaluation of Steel Welded Joints*, International Journal of Fatigue, **26**(12), pp. 1277-1293, 2004.

[9]     Zhao, Z. & Haldar, A., *Bridge Fatigue Damage Evaluation and Updating Using Non-destructive Inspections*, Engineering Fracture Mechanics, **53**(5), pp. 775-788, 1996.

[10]    Asmara, E., *Steel Truss Upperstructure Bridges Assessment Method with Fracture Critical Member Approach (Case Study in Bandar Kota Kediri Bridge)*, Thesis, Department of Civil Engineering, Sebelas Maret University Surakarta, 2012. (Text in Indonesian)

[11]    Ministry of Transportation, Republic of Indonesia, *Circular No. SE.02/AJ.108/DRJD/2008 concerning Guidelines for Maximum Calculation of Amount of Weight Permitted and (Amount of Combined Weight Allowable for Cars of Goods, Special Vehicles, Towing Vehicles and Attachments)*, 2008.

[12]    Paris, P. & Erdogan, F., *A Critical Analysis of Crack Propagation Laws,* Journal of Basic Engineering, **85**(4), pp. 528-534, 1963.

[13]    Fisher, J.W., *Fatigue and Fracture in Steel Bridge-Case Studies*, 1st John Willey & Son, Washington USA, 1984.

[14]    Miner, M.A., *Cumulative Damage in Fatigue,* J. Appl. Mech., pp. 159-164, 1945.

[15]    National Standardization Agency of Indonesia, *SNI 1729-2015: Bridge Loading Standard*, pp. 16-25, 2016. (Text in Indonesian)

[16]    Banvillet, A., Lagoda, T., Macha, E., Nieslony, A., Palin-Luc, T., Vittori, J.F., *Fatigue Life Under non-Gaussian Random Loading From Various Models*. Int J Fatigue., pp. 349-469, 2004.

[17]    Fatemi, A. & Yang, L., *Cumulative Fatigue Damage and Life Prediction Theories: A Survey of the State of the Art for Homogeneous Material*. Int J Fatigue, **20**(1), pp. 9-34, 1998.

[18]    Halford, G.R., *Cumulative Fatigue Damage Modeling-Crack Nucleation and Early Growth*, Int J Fatigue, pp. 256-260, 1997.